FUNCTIONAL ENHANCEMENTS WITHIN ULTRASONIC GAS FLOW MEASUREMENT

Per Lunde, Christian Michelsen Research AS, Bergen, Norway.
Kjell-Eivind Frøysa, Christian Michelsen Research AS, Bergen, Norway.
John Bjørn Fossdal, Kongsberg Metering, Kongsberg, Norway.*
Tom Heistad, Kongsberg Metering, Kongsberg, Norway.*
**) a business unit of Kongsberg Offshore a.s*

SUMMARY

Results and progress from an ongoing R&D program related to the Kongsberg Metering MPU 1200 multipath ultrasonic gas flow meter are presented. The results are outcomes of an R&D Joint Industry Programme (JIP) conducted by Kongsberg Metering (KOS) in a cooperation with Christian Michelsen Research AS (CMR), Statoil, Norsk Hydro and Phillips Petroleum Company Norway, and supported by the Research Council of Norway. The JIP addresses three main topics: (1) calculation of gas density from the measured sound velocity, (2) operation at complex installation conditions (with disturbed flow velocity profiles), and (3) measurement of wet gas.

1. INTRODUCTION

Multipath ultrasonic transit time meters for gas flow measurement (USM) have been developed to a stage where they can be considered as alternatives to the more conventional orifice plate and turbine meters for fiscal metering. As compared with more conventional meters, the USM technology offers significant advantages such as compactness, bi-directionality, short upstream and downstream requirements with respect to bends, no pressure loss, fast response, and large turn-down ratio (1:50). Measurement possibilities are provided which have not been available earlier, such as process monitoring (e.g. pulsating flow, gas quality), and self-checking capabilities. The first generation of ultrasonic meters have been on the market for about 5-10 years, and have demonstrated their capability to provide metering accuracy within national regulation requirements. In appropriate applications, multipath ultrasonic meters offer cost benefits. Although there still remains some hesitation in applying the technology for fiscal and sales gas metering until wider experience has been obtained, and industry standards have been established [1], [2], USM technology is increasingly gaining acceptance throughout the industry, and is today in use in gas metering stations onshore and offshore.

In addition to work related to the accuracy and robustness of such meters for fiscal metering applications (flow velocity metering) [2], there is currently an interest in exploiting the potentials of such meters for additional applications. From 1997 to 1999, an R&D Joint Industry Programme (JIP) is being conducted by Kongsberg Metering (KOS) in a cooperation with Christian Michelsen Research AS (CMR), Statoil, Norsk Hydro and the Research Council of Norway [3]. The JIP addresses three main topics: (1) calculation of gas density from the measured sound velocity, (2) operation at complex installation conditions (with disturbed, non-ideal flow velocity profiles), and (3) measurement of wet gas flow. In the wet gas project Phillips Petroleum Company Norway is also a partner. Results and progress from the ongoing R&D programme related to the KOS MPU 1200 multipath ultrasonic transit time gas flow meter[1] are presented in the following.

2. DENSITY METERING USING THE VELOCITY OF SOUND

In conventional ultrasonic gas flow metering, the USM measures the flow velocity. Through external input of the pressure (P), temperature (T) and compressibility factor (Z), the volume flow rate at standard reference conditions can be found. In order to measure the mass flow rate of gas, the density is measured externally typically either by a density meter or by gas chromatography. This conventional technique is illustrated in Fig. 1. In addition to the measurement of flow velocity and flow rate, the USM also gives a measurement of the velocity of sound in the gas. Traditionally, the measured velocity of sound has only been used for quality check of the meter. This has been done either by comparison of the measured velocity of sound of the various acoustic paths of the meter, or by comparison of the measured velocity of sound with an externally estimated velocity of sound (for example estimated from the output of a gas chromatograph).

1 From October 1998, Kongsberg Metering's FMU 700 multipath ultrasonic tranit time gas flow meter has been denoted MPU 1200.

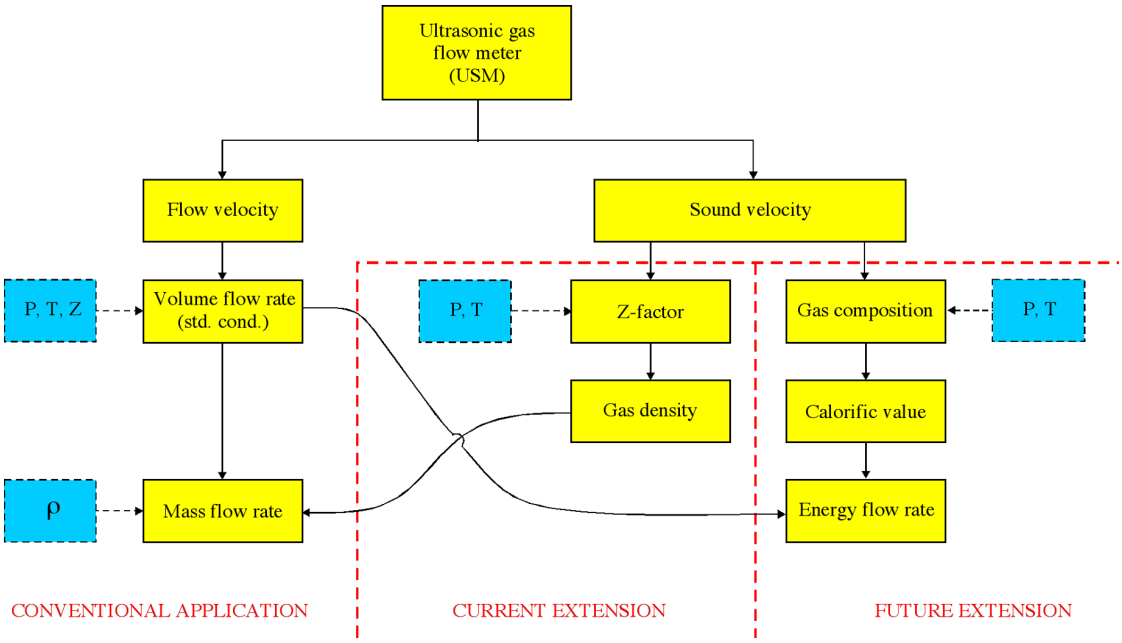

Fig. 1 Illustration of the principles of conventional USM flow metering and the current and future extensions of such metering.

In 1995, Sakariassen [4] described a method of calculating the velocity of sound based on a relationship between pressure, temperature and density. When the USM is installed close to a density meter, such a relation can be used as a quality check of the USM. The velocity of sound calculated from the density can be compared to the velocity of sound measured by the USM. If the deviation between these two estimates of the velocity of sound is too large, it may indicate that the USM may not be working properly.

In his 1995 paper, Sakariassen also hints at finding the relationship to calculate density from the velocity of sound. Such a method will mean that the mass flow rate through a USM can be measured without any external density metering.

Watson [5] and Beecroft [6] have reported attempts to establish such algorithms for calculating the density from the velocity of sound. Watson reports that an algorithm for estimation of density from velocity of sound has been established for gases with methane content greater than 80 %. This algorithm requires the input of an approximate gas composition. Beecroft reports a work based on empirical data from the Trent and Tyne fields, where USMs have been installed and where the density has been measured externally. In his paper, Beecroft states that "currently, knowledge of the gas composition is required to allow an accurate calculation of density, and is likely to remain that way for the foreseeable future".

In parallel to the works reported by Watson and Beecroft, the present JIP has addressed establishing of algorithms for estimating the density from the velocity of sound and the velocity of sound from the density [7]. Such methods may make the USM into a mass flow meter, possibly at a reduced accuracy as compared to the conventional way of measuring the mass flow. This is illustrated as the current extension in Fig 1. The work has been based on an equation of state, and the theoretical relations between the gas compositions, pressure,

temperature and the velocity of sound of natural gas. In addition, general knowledge on natural gas compositions has been used. An uncertainty analysis has been carried out for the established algorithm. In addition, experimental work has been performed to analyze and improve the velocity of sound measurement in the USM. Finally, the established algorithm has been tested experimentally in an explicit flow test. This work is described in the following.

2.1 Model description

A theoretical model for calculating the density from the velocity of sound for a natural gas has been established. The model uses the AGA-8-94 equation of state [8] but is not dependent on this equation of state. A possible future change of equation of state in the theoretical model can be done with just minor model development. At present, the theoretical model requires the following input:

- Pressure at line conditions (external measurement).
- Temperature at line conditions (external measurement).
- Velocity of sound at line conditions (USM measurement).
- Molar fractions of N_2, CO_2, H_2O and H_2S (external measurement / estimate).

Generally, this information is not sufficient to identify the density uniquely. Therefore, assumptions have to be made in order to pick out the "correct" density for a given set of input parameters. These assumptions are related to the likelihood of appearance of the various gas components. For example: consider the following two natural gases: (1) 95 % methane and 5 % propane; (2): 80 % methane, 10 % ethane, 5 % propane and 5 % higher hydrocarbons. Both gases contain 5 % propane, but the second gas is much more likely to appear in pratice than the first gas. From such general guidelines, the "correct" density is chosen.

There are, however, cases where a heavy and a light gas have the same velocity of sound, and where the general guidelines referred to above, give no information on which of these two gases that should be chosen. This can typically be the case for the combination of elevated pressures (typically above 100 bar) and low temperatures (typically below 10 ∞C). In order to reduce such potential problems, the user can specify an interval in which the molar weight of the gas will lie.

The theoretical model can be implemented in an ultrasonic flow meter without any hardware changes. Thus, update of existing flow meters is possible.

In addition to the model for density estimation mentioned above, a model for estimation of the velocity of sound has been established, using the same input as the density model (except that input velocity of sound is replaced by input density). As mentioned above, such a model is to be applied for quality check of a USM that already is installed close to a density meter. Like the model for estimation of density, this model uses the AGA-8-94 equation of state. Also the same guidelines for the gas components are used in the two models. In the model for estimation of the velocity of sound, however, there is no need for specification of an interval for the molar weight of the gas.

2.2 Sensitivity analysis

The input values of pressure, temperature, velocity of sound and molar fraction of N_2, CO_2, H_2O and H_2S to the model of estimation of the density of a natural gas, are associated with input uncertainties. In addition, the guidelines for the gas components in the determination of the "correct" density (described above) are associated with uncertainties that are gas dependent. A sensitivity analysis has been carried out to study the influence of these input uncertainties on the uncertainty of the estimated density [9].

Generally, the uncertainty of the estimated density due to uncertainties in the input parameters will vary with pressure and temperature, and also to some extent with the type of natural gas. As an example, results from an uncertainty analysis based on a typical Åsgard gas composition will be referred. This gas is quite typical with respect to uncertainties in the input parameters, and generality should therefore be assured. The temperature range that has been considered in this uncertainty analysis is –10 °C to 70 °C. The pressure range is 10 bar to 200 bar.

A standard uncertainty of 0.5 % in the input N_2 component (which means that for example 1% is used instead of 0.5 %) will for pressures below 100 bar contribute (isolated) with a standard uncertainty in the density of less than 0.2 %, and in most cases much less than 0.2 %. For pressures above 100 bar, one can expect large standard uncertainty in the density (typically 1 % or larger) for temperatures below 25 °C, while at higher temperatures, the standard uncertainty will typically be less than 0.2 %. The standard uncertainty of the input CO2 component contributes almost exactly in the same way as the standard uncertainty of the input N_2 component.

A standard uncertainty of 0.5 m/s in the measured velocity of sound will contribute (isolated) with 0.4 % or less to the standard uncertainty of the density. Application of an uncertainty model (VESUM) for measurement of the velocity of sound by a USM, indicates that a standard uncertainty at this level, or better, is within reach, especially at dimensions of 12" and larger [10].

The pressure and temperature uncertainties will in practice contribute less to the uncertainty in density than the uncertainty in the inert gas compositions and the velocity of sound do. The uncertainty analysis indicates that the velocity of sound measurement must be relatively good (standard uncertainty of about 0.5 m/s or less), in order to provide a relatively accurate density estimation. The uncertainty of the N_2 and CO_2 content indicates that in practice, a good density estimate can be obtained if the content of N_2 and CO_2 does not vary more than some tenths of a percent. At Åsgard, for example, the N_2 fraction is about 0.7 %. Then variations from say 0.5 % to 0.9 % can be tolerated without updating the input molar fraction of N_2. Similar tolerances exist for CO_2, H_2O and H_2S.

In addition to the uncertainties of the input parameters to the algorithm, the guidelines for the gas components in determining the "correct" density will introduce uncertainties that are gas dependent. For the Åsgard field this standard uncertainty is quite small, below 0.1 % except for the region where the pressure is above 120 bar and the temperature is below 20 °C. For other fields, this uncertainty contribution can typically be some tenths of a percent. An evaluation of this uncertainty contribution is possible before installation at a specific gas field. With stable N_2 and CO_2 content, and with a good velocity of sound measurement, it

should for many gas fields be possible to obtain the density with a relative expanded uncertainty of about 0.5 % or less (95 % confidence interval). Other gas fields will give a larger uncertainty. Therefore, in most cases an expanded uncertainty of 0.5 – 1 % or better should be within reach.

2.3 Flow testing and results

The two algorithms for calculating the density from the velocity of sound, and the velocity of sound from the density, have been implemented in a 6" MPU 1200, and a flow test at Statoil's K-Lab was carried out in April 1999 to test the algorithms. The reference density at K-Lab was calculated from the output of a gas chromatograph. The input N_2 and CO_2 values to the algorithms are taken from the same gas chromatograph. At K-Lab, only one gas composition was available. This gas composition is (by chance) relatively well suited for the general guidelines for the gas components in the determination of the "correct" density, but not perfect in this respect. In order to test the algorithm at various densities, two temperatures (about 30 °C and 50 °C) and two pressures (about 30 bar and 80 bar) were used. For each of the four P, T – combinations, the flow velocities 5 m/s, 10 m/s and 20 m/s were tested in order to demonstrate flow independence of the algorithms as implemented in the USM. The results from the K-Lab test are shown in Fig. 2, where the deviation between the density as calculated from the measured velocity of sound and the reference density is shown for each P, T, v combination. Typically, in this test, the density has been measured by the USM to within ±0.1 % of the reference density.

2.4 Perspectives (planned work)

In future this work is planned to be extended in two ways:

As stated in Section 2.2, the algorithms do not work properly on all gas compositions, due to the guidelines for the gas components in the determination of the "correct" density. More robustness is planned to be built in here, especially in cases where some rough knowledge on the gas composition is available.

In previous work at CMR, it has been demonstrated that the calorific value can be found from the velocity of sound and additional measurements. It is planned to design an algorithm well suited for USMs based on these results. This may give possibilities to also measure the energy flow rate using USM, as illustrated as a future extension in Fig. 1.

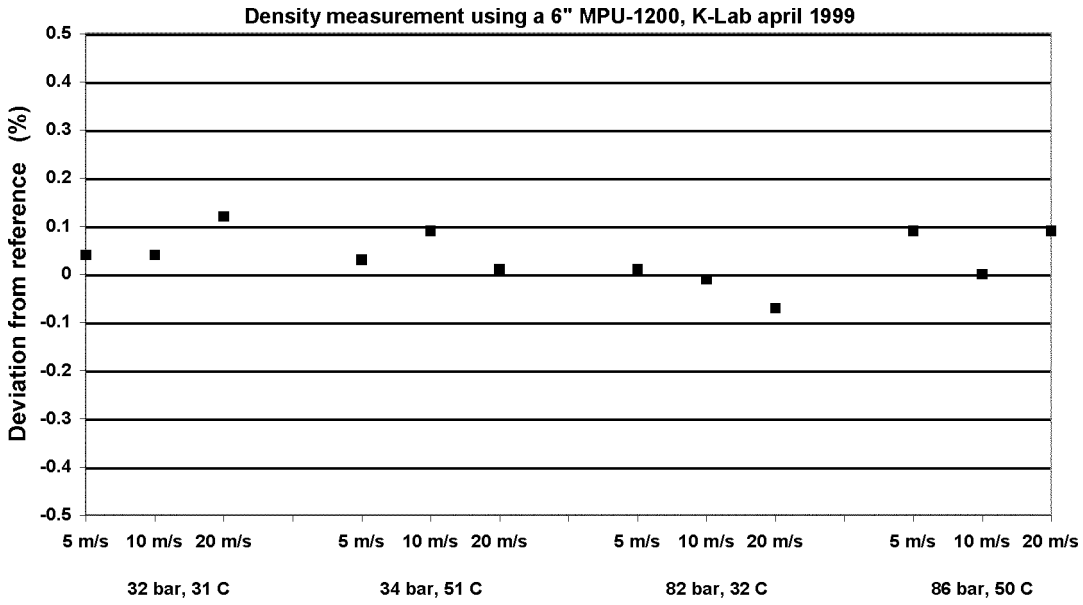

Fig. 2 Results from the online test of the density algorithm at K-Lab using a 6" MPU 1200.

3. INSTALLATION EFFECTS

In compact metering stations, with the flow meter possibly installed close to bend configurations, the flow profile can be quite complex, with an asymmetric axial flow profile, and also significant asymmetric transversal flow components. In the present JIP, the performance of the MPU 1200 ultrasonic meter has been studied at a wide range of complex flow profiles, both numerically calculated (CFD) and experimentally established (flow tests). These results have been used to improve the meter's integration of the flow velocity over the pipe cross section, to obtain improved measurement accuracy for meters installed close to bends. Results from the testing of an improved MPU 1200 integration algorithm are presented.

As a background, in order to describe the problem of non-ideal flow, consider a single acoustic path (non-bouncing) with interrogation length Li and an angle fi to the axial direction. First, if the average flow velocity along acoustic path no. i is purely axial with value , the upstream and downstream transit times can, to the lowest approximation in the Mach number, be written as

$$t_{1i} = \frac{L_i}{c - \bar{v}_{i,A}\cos\phi_i}; \qquad t_{2i} = \frac{L_i}{c + \bar{v}_{i,A}\cos\phi_i} \tag{1}$$

where c is the velocity of sound. The average axial flow velocity along acoustic path no. i can be found as

$$\bar{v}_{i,A} = \frac{L_i\left(t_{1i} - t_{2i}\right)}{2t_{1i}t_{2i}\cos\phi_i} \tag{2}$$

which is the formula (or a variant of the formula) used for calculating the average axial flow velocity along the acoustic path. However, when an average transversal flow component along the acoustic path, $\bar{v}_{i,T}$, is present (see Fig. 3), the transit times are changed to

$$t_{1i} = \frac{L_i}{c - \bar{v}_{i,A}\cos\phi_i - \bar{v}_{i,T}\sin\phi_i}; \qquad t_{2i} = \frac{L_i}{c + \bar{v}_{i,A}\cos\phi_i + \bar{v}_{i,T}\sin\phi_i} \tag{3}$$

and the estimated flow velocity will be

$$\bar{v}_{i,A} + \bar{v}_{i,T}\tan\phi_i = \frac{L_i\left(t_{1i} - t_{2i}\right)}{2t_{1i}t_{2i}\cos\phi_i} \tag{4}$$

Thus, transversal flow components will influence on the measured flow velocity along a single path. If not eliminated or corrected for, these contributions give measurement errors.

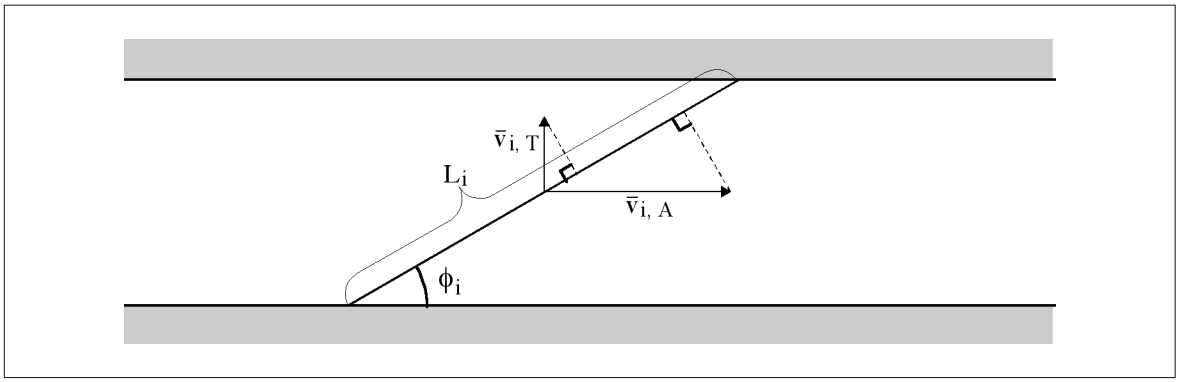

Fig. 3 The influence of axial and transversal flow components on a single acoustic path illustrated by decomposition of the flow velocities along the acoustic path.

In a multipath USM, the measured flow velocities from the individual acoustic paths are combined to obtain an average axial flow velocity over the pipe cross section. This process is denoted the integration method for the specific USM. A good integration formula should fulfil two requirements:

- Integrate the axial flow velocity to a sufficiently high accuracy.
- Eliminate as good as possible the influence of the transversal flow components.

Transversal flow components will occur especially when the USM is installed downstream bends and other obstructions of the pipe flow. It is expected that downstream a double bend out of plane, the transversal flow regime is typically a swirl, while downstream a single bend, a cross flow is typically established, see Fig. 4. As demonstrated above, such transversal flow components can contribute to the flow measurement performed by each acoustic path. There are examples from installations downstream double bends out of plane where the transversal flow components can be 10 % of the axial flow component, or larger. In order to handle such transversal flow components, a USM needs to compensate for the appearance of such components, either by measuring the transversal component or by indirect compensation. Such indirect compensation can for example be that symmetric cross flow will be automatically compensated for through the geometrical configuration of the acoustic paths (contribution to one acoustic path is equal in magnitude but of opposite sign of the contribution to an other acoustic path). Thus, a careful design can in some cases cause the

effect of the transversal flow components to cancel between the various acoustic paths. However, in practice, the transverse flow components often will neither be a symmetric swirl nor a symmetric cross flow, but instead some kind of an asymmetric variant of either swirl or cross flow, or something in between.

In the JIP, a review of the integration method used in a 6-path USM has been performed after gaining experimental experience (flow testing) of this type of meter for about 4 years. The work has lead to a further optimization of the integration method used in the meter, based among other on the set of experimental flow test data, and thus to an improved performance of the meter.

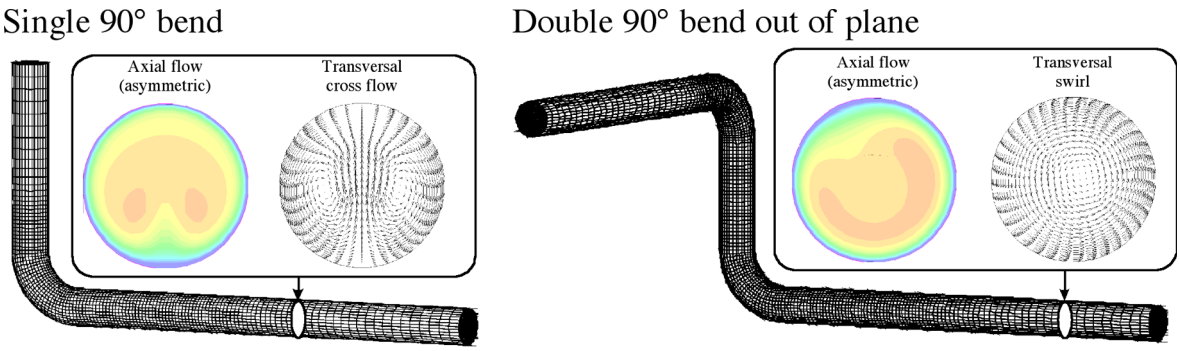

Fig. 4 Illustration (CFD calculations) of typical cross flow (left pipe configuration) and swirl (right pipe configuration) flow regimes.

3.1 Experimental input (flow testing)

From the first tests in 1995 [11], the 6-path USMs have been flow tested at various flow laboratories. In the study presented here, a selected set of experimental data, gathered in the period 1995 to 1998, has been used as a basis. These include the following installations:

- Baseline tests with 40 to 100 diameters straight pipe upstream the USM.
- Baseline tests with flow conditioners upstream the USM.
- Installation tests with a single 90° bend upstream the USM.
- Installation tests with a double 90° bend out of plane upstream the USM.
- Installation tests with a U-bend upstream the USM.

The experimental input data used in the present study come from flow tests at

- Statoil's K-Lab, Norway
- Ruhrgas' Lintorf HP test facility, Germany
- Gasunie's Bernoulli Laboratory, Westerbork, The Netherlands
- Southwest Research Institute, Texas, USA
- Offshore installation at Oseberg, Norway

The experimental data set from these flow tests constitutes the major basis for the integration model development which is done under the present project. In addition, complementary results using computer simulations have been used to some extent. The computer simulations are discussed below.

3.2 Modelling

As stated above, a good integration method must integrate the axial flow profile sufficiently well, in addition to reduce the influence of the transversal flow components as much as possible. The axial flow profile integration used up to now in the 6-path USM is based on a well established mathematical / numerical algorithm, and has demonstrated to integrate well both symmetric and asymmetric axial flow profiles. In the modification work, it has therefore been essential that in the case of no transversal flow components in the pipe, the modified integration method should give the same answer as the method currently implemented in the USM.

In order to obtain an improved cancellation of the transversal flow components, knowledge on the asymmetry in these components has to be established. This knowledge on asymmetric transversal flow components has been established through careful studies of the experimental data available from flow tests. In addition, two simulation tools developed at CMR have been used. First, the computational fluid dynamics (CFD) code MUSIC is used to simulate the pipe flow through and downstream various bend configurations. Thereafter, an updated draft version of the USM uncertainty model GARUSO has been used to calculate the flow velocity estimated by each acoustic path in a USM, and the contribution to these flow velocities from the axial and the transversal flow components in the pipe flow. Thereafter, the average axial flow velocity as estimated by the USM is compared to a reference value that is also calculated by the program. In this way, a numerical "flow test laboratory" has been established.

The CFD flow simulations have been carried out for the following 4 types of pipe geometry:
- Single 90° bend.
- Double 90° bend out of plane, no separation between the bends.
- Double 90° bend out of plane, 3 inner diameters separation between the bends.
- Double 90° bend out of plane, 10 inner diameters separation between the bends.

For each of the geometries, three different inlet flow conditions have been chosen for the pipe work in the CFD simulations. This has been done because in practice, the inlet conditions on a bend configuration may be far from an ideal, fully developed turbulent axial flow profile with no transversal flow components. By using several inlet flow conditions, the robustness of USMs against such variations in inlet conditions can to some extent be studied.

For the single bend conditions, the following three inlet flow conditions have been used:
- Fully developed symmetrical axial flow profile (power law profile) with no transversal flow components.
- Fully developed symmetrical axial flow profile (power law profile) with a superposed symmetric swirl, and a maximum transversal flow component of about 5 % of the axial flow component.
- Fully developed symmetrical axial flow profile with a superposed cross flow.

For each of the double bend out of plane geometries, the following three inlet flow conditions have been used:
- Fully developed symmetrical axial flow profile (power law profile) with no transversal flow components.

• Fully developed symmetrical axial flow profile with a superposed symmetric swirl, with a maximum transversal flow component of about 10 % of the axial flow components. Rotation of swirl in positive and negative direction.

In addition, each of these flow simulations has been carried out at the two Reynolds numbers 105 and 107. This gives a total of 24 different flow situations that have been analyzed. For each of these 24 cases, virtual USMs with various acoustic path configurations have been "installed" 5 D, 10 D, 15 D and 20 D downstream the bends. The flow velocity estimated by each acoustic path in a USM, and the contribution to these flow velocities from the axial and the transversal flow components in the pipe flow, are then calculated. At every (virtual) USM installation point, the USM has been rotated from 0° to 360° in steps of 5° in order to see the influence of various orientations of the meter.

3.3 Integration method

By analyzing the experimental (flow testing) and numerical (simulation) data, some candidate models for the asymmetry in the transversal flow components have been established. These asymmetry models lead to candidate integration models for obtaining the average axial flow velocity from the flow velocities estimated by each acoustic path. The candidate integration models use the same input as previous models (i.e. the measured flow velocity at each of the 6 acoustic paths). This means that no hardware changes are necessary, and therefore also updating of existing 6-path USMs to the new models is possible. The integration of the axial flow profile (symmetric or asymmetric) is performed exactly as earlier. This means that the new candidate integration models should provide improved results in installation tests, while the baseline test results should remain about unchanged, when compared to the existing integration method in the 6 path USM. In the present paper, results using one of these candidate integration models will be shown. The integration model to be implemented in the MPU 1200 is to be chosen in the near future.

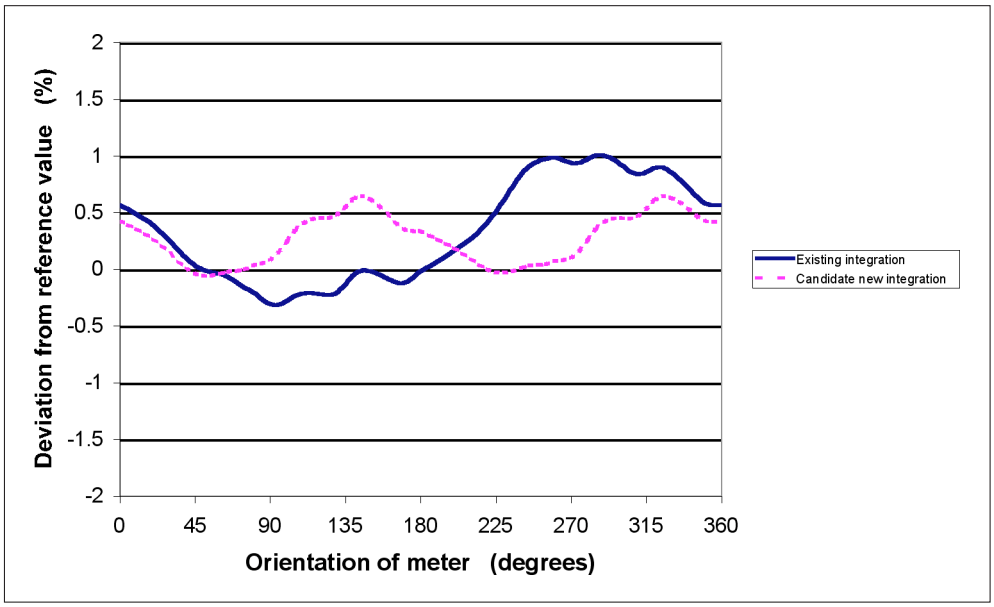

Fig. 5 Example of calculated deviation from reference (simulation results) for a 6-path USM using the existing and the candidate new integration method. In this example, the USM is "installed" 10D downstream a double bend out of plane with 3D separation between the bends and a rotational inlet flow on the bends. Results for various orientations (rotations) of the USM are shown.

As an example of the existing and the candidate new integration method, a GARUSO simulation based on MUSIC CFD input is shown in Fig. 5. Here the deviation between the USM output and the reference flow velocity is calculated for various orientations of the meter spool in the pipe, when the USM is rotated from 0° to 360°. The installation is 10D downstream a double bend out of plane with 3D separation between the bends, and with a rotational inlet flow to the bends. It is seen that the candidate new integration model will reduce the span of the deviation over the various orientations of the meter from about 1.3 % for the existing model to about 0.7 % for the candidate new model. In this context it should be noted that all USMs show some dependency of the orientation of the meter. This has been demonstrated experimentally in flow tests of various meter types (4 - path, 5 - path and 6 - path meters), see e.g. [12], [13]. Such orientation effects should be reduced as much as possible.

3.4 Flow testing and results

The new candidate integration method has been developed based on experimental data from pre-1999 flow tests and CFD data. The method is then tested in two new flow tests as part of a verification. The first test is designed especially for the integration method project. In this test, a 6" MPU 1200 was used. The test was carried out at Statoil's K-Lab in June 99. The second test was carried out by Southwest Research Institute (SWRI) and Gas Research Institute (GRI) on a 12" MPU 1200 in August 99. This test was part of a larger test where three commercially available USMs were tested [12], [13]. The 12" MPU 1200 was equipped with the old integration method. In both tests, the candidate new integration method was tested through postprocessing of the experimental data.

Fig. 6 Installation of a 6" MPU 1200 at Statoil's K-Lab 10D downstream a single 90∞ bend. A flow conditioner is mounted in the read flange upstream the single bend. Photograph provided by Statoil K-Lab.

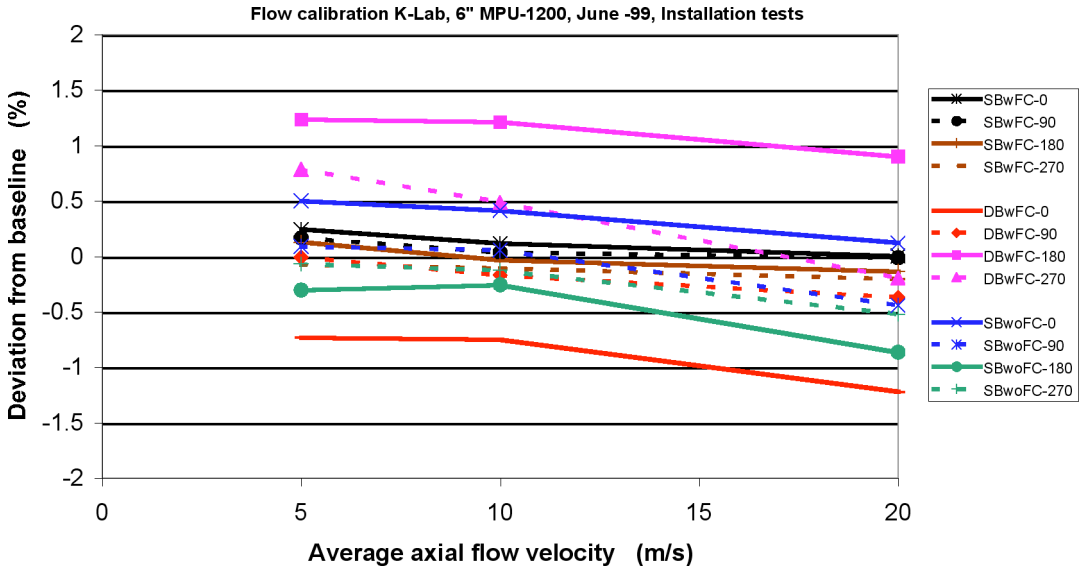

Fig. 7 The deviation from baseline tests for installation tests of a 6" MPU 1200 at K-Lab in June 1999 using the existing integration method of the meter. Legend text: SBwFC: MPU 1200 installed 10D downstream a single bend with K-Lab flow conditioner installed upstream the bend. DBwFC: MPU 1200 installed 10D downstream a double bend out of plane with K-Lab flow conditioner installed upstream the bends. SBwoFC: MPU 1200 installed 10D downstream a single bend with no flow conditioner installed upstream the bend. 0, 90, 180 and 270 refer to orientation (rotation) of the meter in degrees relative to a normal installation of the meter with the electronics on top of the meter.

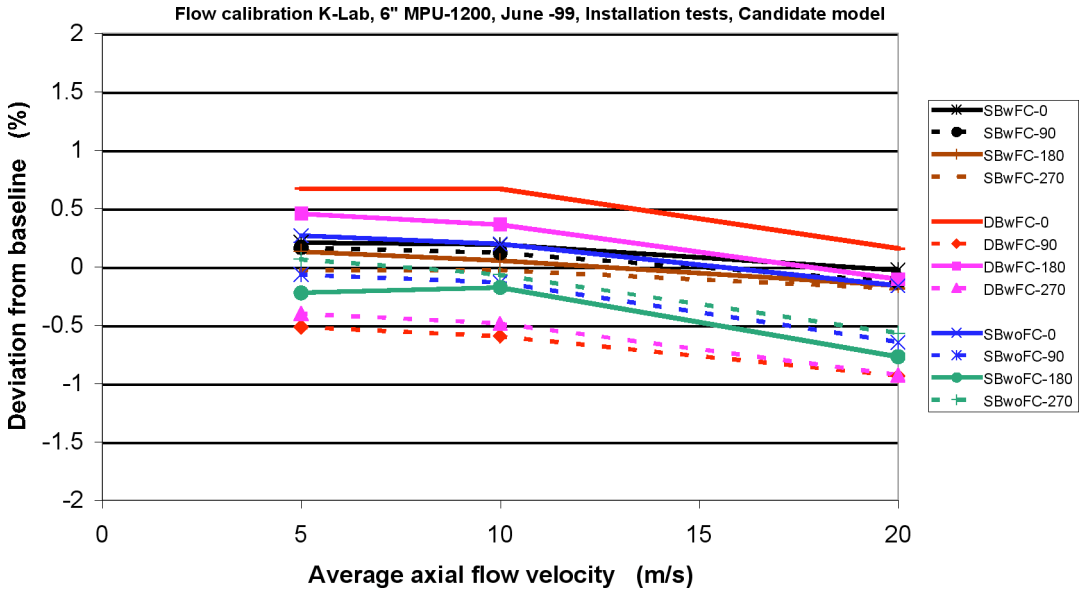

Fig. 8 Same as Fig. 7, except that the candidate new integration method has been used instead of the existing integration method of the MPU 1200.

At Statoil's K-Lab, 4 types of installations were tested:
- Baseline tests with the USM located about 40 D downstream a K-Lab flow conditioner.
- Installation tests 10D downstream a single 90° bend. A K-Lab flow conditioner was installed upstream the bend.
- Installation tests 10D downstream a double 90° bend out of plane. A K-Lab flow conditioner was installed upstream the bends.
- Installation tests 10D downstream a single 90° bend. No flow conditioner was installed.

For each of these 4 installations, the meter was tested in 4 different orientations (0°, 90°, 180° and 270° rotation) of the meter, relative to the normal installation orientation (with the electronics at the top of the meter). Three flow velocities, 5 m/s, 10 m/s and 20 m/s, were used in each installation test.

Upstream the single or double bend in the installation tests, there are several other bends, as can be seen on Fig. 6. Therefore, the inlet flow profile on the single or double bend can be quite complex. Therefore, a flow conditioner was installed upstream the single / double bend. This was done to ensure that the measured installation effects on the USM were due to the bend configuration in question. In addition, single bend tests were also carried out without a flow conditioner upstream the bend, in order to investigate effects of various inlet flow conditions. The average flow velocities measured by the 6 acoustic paths demonstrate that the inlet flow profile on the single bend may be an important parameter when flow calibrations take place.

In Figs 7 and 8, the deviation from baseline measurements has been shown for the installation tests. This presentation form has been chosen because the deviation from baseline demonstrates the influence of the bend configuration as compared to a baseline condition. Results using both the existing MPU 1200 integration method and the candidate new integration method are shown. It can be seen that the spread of the results is larger for the existing method than for the candidate new model.

At SWRI, a 12" MPU 1200 was tested in the following installations:
- Baseline tests 100D downstream a single 90° bend, without flow conditioner between the bend and the meter.
- Installation tests 10D and 20D downstream a single 90° bend, with no flow conditioner between the bend and the meter.
- Installation tests 10D and 20D downstream a double 90° bend out of plane, with no flow conditioner between the bends and the meter.
- Installation tests 10D and 20D downstream a double 90° bend in plane, with no flow conditioner between the bends and the meter.
- Baseline tests and installation tests with flow conditioners (of various types) between the bend and the meter.

For each installation test, the meter has been tested with two orientations (0° and 90° rotation). Upstream the bends, a Gallagher flow conditioner has been installed [13]. The MPU 1200 was equipped with the existing integration method. The data from each acoustic path have, however, kindly been made available to the present project by T. Grimley, SWRI, enabling testing of the candidate new integration model through postprocessing. In Fig. 9, the deviation from reference has been shown for the flow tests at SWRI (with the existing integration method), for all flow tests

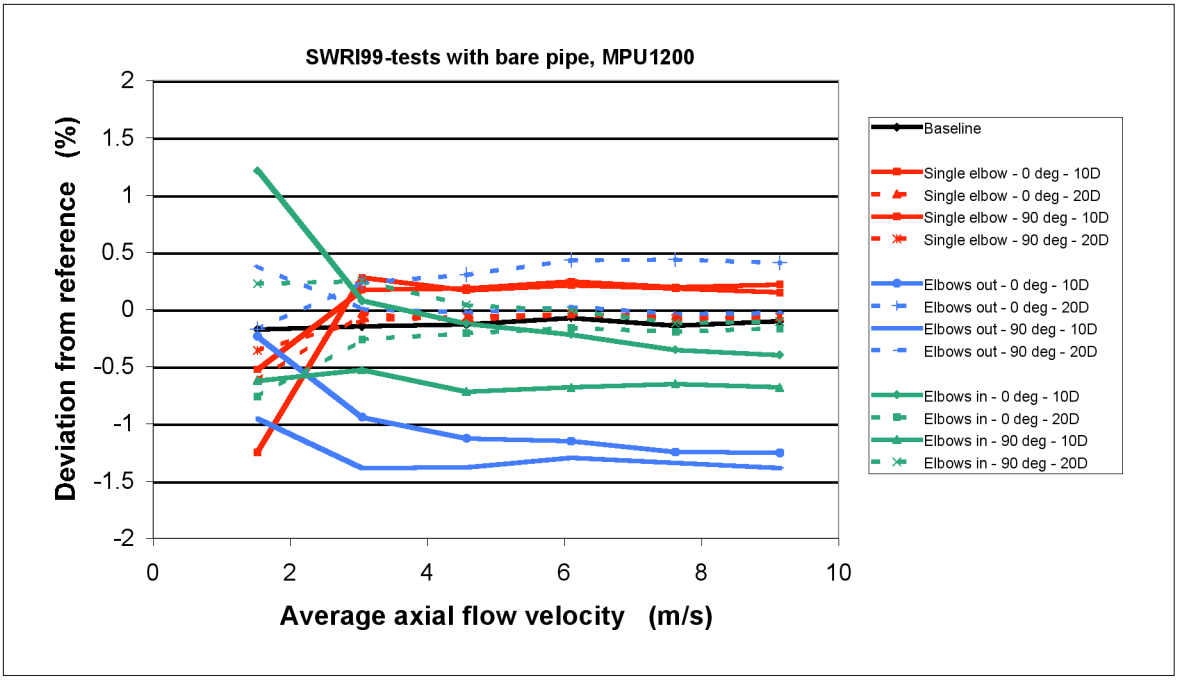

Fig. 9 The deviation from the reference measurement for a 12" MPU 1200 installed 10D and 20D downstream a single 90∞ bend (single elbow), a double 90∞ bend out of plane (elbows out) and a double 90∞ bend in plane (elbows in). Orientation of the meter is 0∞ and 90∞. Existing integration formula used.

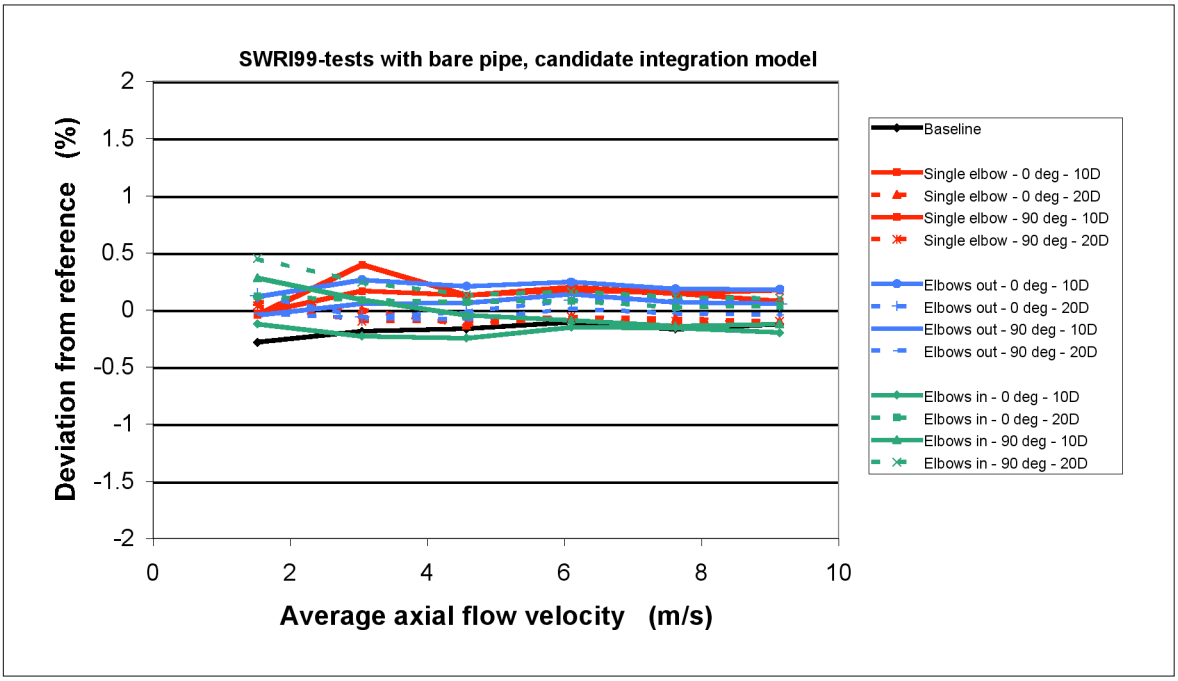

Fig. 10 Same as Fig. 9 except that the candidate new integration model is used through postprocessing of the experimental data (using the same data as used as basis for Fig. 9).

Table 1 Flow weighted mean error for installation tests of a 12" MPU 1200 at SWRI using bare tube or a flow conditioner (of various types) between the bend and the MPU 1200. Existing integration formula used. Table taken from [13].

	Single Elbow		Elbows Out		Elbows In	
	0	90	0	90	0	90
Bare at 10D	0.14	0.29	-1.02	-1.22	-0.18	-0.52
Bare at 20D	0.03	0.04	0.48	0.12	-0.10	0.10
19 Tube	0.33	0.42	0.09	-0.11	0.14	0.10
Vortab	0.05	0.02	-0.19	-0.19	-0.12	-0.09
Nova 50E	0.02	0.02	-0.42	-0.64	-0.18	-0.14
Nova 50E @ 3D	-0.05	0.15	-0.38	-0.69	-0.17	-0.16
GFC	0.24	0.15	-0.13	-0.11	0.06	0.08

Table 2 Same as Table 1 except that the candidate new integration model is used through postprocessing of the experimental data.

	Single Elbow		Elbows Out		Elbows In	
	0	90	0	90	0	90
Bare at 10D	0.29	0.30	0.35	0.22	-0.04	0.08
Bare at 20D	0.08	0.06	0.20	0.11	0.20	0.30
19 Tube	0.31	0.38	-0.13	0.10	0.13	0.10
Vortab	0.07	0.01	0.10	0.12	-0.08	-0.03
Nova 50E	0.01	-0.01	-0.27	-0.23	-0.24	-0.18
Nova 50E @ 3D	-0.02	0.15	-0.22	-0.23	-0.26	-0.24
GFC	0.25	0.14	-0.12	-0.09	0.04	0.08

Table 3 Same as Table 1 except that the candidate new integration model is used through postprocessing of the experimental data and that the numbers are relative to the reference meter at SWRI and not relative to the baseline tests.

	Single Elbow		Elbows Out		Elbows In	
	0	90	0	90	0	90
Bare at 10D	0.14	0.15	0.20	0.07	-0.19	-0.07
Bare at 20D	-0.08	-0.09	0.05	-0.04	0.05	0.15
19 Tube	0.15	0.21	-0.29	-0.06	-0.03	-0.06
Vortab	-0.15	-0.21	-0.13	-0.11	-0.30	-0.26
Nova 50E	0.03	0.01	-0.25	-0.21	-0.22	-0.16
Nova 50E @ 3D	0.16	0.33	-0.04	-0.05	-0.08	-0.06
GFC	0.15	0.04	-0.22	-0.18	-0.05	-0.01

without flow conditioner between the bend and the flow meter. It can be seen that there is a span of about 2 % between the various curves. In addition, the linearity of the individual curves is not good at low flow velocities. In Fig. 10, the similar deviation from reference has been shown when postprocessing the same data set using the new candidate integration method. It can be seen that all curves now are well within ±0.5 % deviation from the reference meter. This indicates that the asymmetry model for the transversal flow components, which is a part of the candidate new integration model, represents a better performance of the MPU

1200 downstream bend configurations. It should be noted that the results from the K-Lab and the SWRI - tests have not been used in the development of the candidate integration method.

The results of the tests of the MPU 1200 meter have been summarized by Grimley [13] in Table 1. Each number in this table represents a flow weighted mean error for a specific installation of the meter with or without flow conditioner. The numbers are given relative to the baseline measurements. In Table 2, similar numbers are calculated for the candidate new integration model. It is seen that generally, the flow weighted mean errors are reduced. In Table 3, the flow weighted mean error is shown when compared to the reference measurements at SWRI (and not to the baseline measurements). It is seen that the highest deviation from reference is 0.33 %.

The flow tests at K-Lab of a 6" MPU 1200 and at SWRI of a 12" MPU 1200 have both shown that the MPU 1200 is less sensitive to installation effects with the candidate new integration method than with the existing integration method. At SWRI, the deviation from reference measurement in the installation tests was less than 0.5 % in all tests. At K-Lab, the deviation was larger. In both tests, the span in deviation between the various installation tests was reduced by using the candidate model instead of the existing integration model.

4. METERING OF WET GAS

As a part of the JIP, the MPU 1200 ultrasonic gas flow meter is being further developed to measure natural gas flow that contains liquid phase contaminants. These liquids contaminants may be either condensate, water, or chemical treatments injected into a pipeline. Up to 5% liquid (by rate, cf. Section 4.1) is often used as tentative maximum wetness figure for such wet gas flow. A 6" wet gas test meter using 3 acoustic paths has been developed by KOS and CMR and is currently being tested in wet gas flow. The first objective is to measure the gas volume flow rate, in spite of liquid contaminants being present, and without kn owing the liquid volume fraction. Possibilities for measurement of the liquid volume fraction using ultrasonic techniques are also addressed in the project (but are not reported here). As a basis for the meter development, experimental and theoretical studies have been conducted, addressing (among others) (a) an uncertainty analysis of wet gas USMs, (b) the influence of wet gas (liquid droplets, liquid film, etc.) on the transmitted and scattered sound field (such as sound velocity, sound attenuation, scattering level, transducer directivity, etc.), and (c) chemical resistance of the transducers. Selected results from this ongoing work are presented in the following.

4.1 Uncertainty analysis

Background. For ultrasonic metering of the gas volume flow rate, a number of factors due to the liquid contaminants in the gas influence on the uncertainty budget of the ultrasonic meter, such as:

(A) Uncertainty of the **gas area** (A_g), i.e. the cross-sectional area occupied by the gas phase in the meter body. This is determined by the uncertainty of the liquid hold-up.

(B) Possible build-up of liquid in the transducer ports, causing an acoustic bridge between the transducers and the steel meter body (**"cross-talk"**), dependent on the self-draining capacity of the transducer ports. An increased level of ultrasound propagating in the meter body acts as noise, causing a reduced signal-to-noise ratio (SNR), which contributes to increase the uncertainty of the transit time determination (relative to in dry gas).

(C) Reduced signal level relative to the dry case, due to **excess sound attenuation** caused by (i) liquid droplets in the wet gas, and (ii) liquid present on the transducer faces. This results in a lower signal-to-noise ratio (SNR), which contributes to increase the uncertainty of the transit time determination (relative to in dry gas).

(D) **Liquid present on the transducer faces,** which causes a shift in the measured transit times. Such liquid may also influence on the transducer directivity and thus the acoustic diffraction correction, causing a larger uncertainty of the transit time determination (relative to in dry gas).

(E) **Path failure** due to possible flooding of the transducers (due to liquid slugs, high liquid volume fraction in horizontal stratified flow, etc.). A single path failure with subsequent meter recovery may not be dramatic, but a failure of all paths will be more serious.

These effects cause additional uncertainty due to wet gas, relative to the uncertainty of the USM in dry gas.

Uncertainty model. In the "GERG project on ultrasonic flow meters" (1995-98) [2], a theoretical uncertainty model for multipath ultrasonic metering of dry gas has been developed, and implemented in a PC program, GARUSO Version 1.0 [14]. The procedure used for evaluating and expressing uncertainties is the procedure recommended by ISO in the "Guide" [15]. The uncertainty model takes into account an extensive set of factors that may contribute to the uncertainty of the ultrasonic measurement, such as the standard uncertainties of gas parameters, geometry parameters, a number of contributions to the measured transit times, and the integration technique. For more details, cf. refs. [14], [2].

Under the present project, the GARUSO uncertainty model has been extended to account for wet gas effects, where the "wet gas contributions" (A)-(D) addressed above have been modelled and built into the uncertainty model, in addition to the "dry gas contributions" referred to above.

It should be mentioned that the uncertainty model takes as a starting point that the meter does function and operate in the wet gas flow, i.e. that acoustic signals are detected on all paths (although the model accounts for low signal-to-noise ratio, SNR). Path failures due to flooding (point (E) above) are not accounted for in the uncertainty model. In practice, path failures may be treated in the meter e.g. by extrapolation procedures based on history and profile information.

Wet gas metering, functional relationship. In a dry gas situation, the average axial gas flow velocity over the pipe's cross-section (at pipe flow conditions), , and the axial gas volume flow rate (at pipe flow conditions), , are given as

$$\bar{v}_g = \sum_{i=1}^{N} w_i \bar{v}_i \,, \tag{5}$$

$$q_g^A = \bar{v}_g A \tag{6}$$

respectively. Here, is the average axial gas flow velocity along the ith acoustic path, given by Eq. (2), and wi is the integration weight factor of the ith path. N is the number of acoustic paths, and A is the pipe's inner cross-sectional area.

In a wet gas situation, the axial volume flow rate of the gas phase (at pipe flow conditions) is given as

$$q_g = \bar{v}_g A_g \tag{7}$$

where

$$A = A_g + A_l \tag{8}$$

and A_g and A_l are the portions of the pipe's cross sectional area which are occupied by the gas and liquid phases, respectively. In wet gas flow, the meter's integration method is here assumed to be the same as in dry gas. The volume flow rate measured by the USM is then

$$q_g^A = \bar{v}_g A = \bar{v}_g (A_g + A_\ell) = q_g \left(1 + \frac{A_\ell}{A_g}\right) \approx q_g (1 + \phi_V), \qquad for\ \phi_V << 1 \tag{9}$$

so that

$$q_g \cup q_g^A (1 - \phi_V) \tag{10}$$

Eq. (10) is the expression used in the USM to calculate the gas volume flow rate in wet gas from the measured transit times.

Here, ϕ_V is the liquid volume fraction, which for a relatively homogeneous multiphase mixture (over the volume V inside the meter body) is approximately equal to the liquid hold-up, i.e.

$$\phi_V \cdots \frac{V_l}{V_g + V_l} \cup \frac{A_l}{A_g + A_l} \cdots \quad \text{liquid hold-up,} \tag{11}$$

which is small in wet gas (i.e.ϕ_V « 1). Vg and V_l are the volumes which are occupied by the gas and liquid phases (at pipe flow conditions), respectively, in the volume $V = V_g + V_l$ inside the meter body.

To avoid confusion, it should be noted that the "liquid volume fraction" ϕ_V as defined here, is in general not equal to the "liquid rate fraction", ϕ_q, defined as

$$\phi_q \equiv \frac{q_l}{q_g + q_l} \tag{12}$$

where q_g and are the volume flow rates of the gas and liquid phases (at pipe flow conditions), respectively. ϕ_q is a quantity which is usually measured in connection with testing of multiphase flow meters (measured e.g. at the gas and liquid injection pipes, or after separation), and is sometimes (misleadingly) referred to as the "liquid volume fraction". The frequently used tentative maximum wetness figure of "5 % liquid" in wet gas flow usually refers to ϕ_q, i.e. $\phi_q < 0.05$.

The two-way relationships between theϕ_V and ϕ_q are

$$\phi_V = \left[1 + \frac{\bar{v}_\ell}{\bar{v}_g}\left(\frac{1}{\phi_q} - 1\right)\right]^{-1}, \qquad \phi_q = \left[1 + \frac{\bar{v}_g}{\bar{v}_\ell}\left(\frac{1}{\phi_V} - 1\right)\right]^{-1}. \tag{13}$$

where $\bar{v}_\ell$ is the average axial liquid flow velocity over the pipe's cross-section (at pipe flow conditions). Two special cases may be of interest. For (the hypothetical) case of no slip , $(\bar{v}_\ell = \bar{v}_q)$, one has $\phi_V = \phi_q$. For wet gas one has $\phi_q \ll 1$ (since $\phi_q < 0.05$), giving ϕ_q (since $\bar{v}_g \geq \bar{v}_\ell$). In this case the relationships (13) reduce to

$$\phi_V \cong \frac{\bar{v}_g}{\bar{v}_l}\phi_q \tag{14}$$

Uncertainty analysis. From Eq. (10), the relative expanded uncertainty of the gas volume flow rate, qg, becomes

ϕ_V is thus in general larger than ϕ_q, and may exceed 5 %. Since the slip ratio $\bar{v}_g/\bar{v}_\ell$ is usually unknown, ϕ_V can not easily be determined from ϕ_q, but may have to be measured separately.

$$E_q = k\sqrt{(E_q^A)^2 + u^2(\hat{\phi}_V)} = k\sqrt{E_m^2 + E_I^2 + u^2(\hat{\phi}_V)} \tag{15}$$

Here, k is the coverage factor ($k = 2$ for a 95 % confidence interval), E_q^A is the relative combined standard uncertainty of the estimate $\hat{q}_g^A$, E_m is the relative combined standard "path uncertainty" of $\hat{q}_g^A$ (accounting for propagation of standard uncertainties of the geometry parameters and transit time contributions), E_I is the relative combined standard "integration uncertainty" of $\hat{q}_g^A$, and $u(\hat{\phi}_V)$ is the standard uncertainty of the estimate $\hat{\phi}_V$ (representing the uncertainty in the measurement of A_g due to the uncertainty of the liquid volume fraction estimate).

Relatively comprehensive expressions for E_m and E_I are given in ref. [14] (derived for dry gas), and will not be repeated here. The same expressions can also be applied to the wet gas case. In case of wet gas, however, E_m becomes larger than in dry gas (especially at low flow velocities), as described in the following for the "wet gas contributions" (A)-(D) discussed above.

Possible increased cross-talk due to liquid build-up in the transducer ports (cf. (B)), contributes in E_q. (15) through E_m (reduced SNR). Increased signal attenuation due to (i) liquid droplets in the gas, and (ii) liquid present on the transducer faces (cf. (C)) also contributes through E_m (reduced SNR). Shift in measured transit times and changed diffraction correction due to liquid present on the transducer fronts (cf. (D)) contribute through E_m as well. The uncertainty of the gas area Ag (cf. (A)) contributes through the term u($\hat{\phi}_V$). Due to space limitations, the details of this analysis will not be given here.

Results. Fig. 11 shows an example of a calculated relative expanded uncertainty, E_q, for a multi-path USM, plotted as a function of the average axial gas flow velocity. The three different curves (a), (b) and (c) are explained in the figure text. The figure demonstrates some characteristic and important results predicted by the uncertainty model, for the "excess uncertainty" due to wet gas relative to the "dry gas baseline uncertainty", (a) (which is taken to be a tentative but typical example).

The "wet gas contributions" (B) and (C) to the USM uncertainty seem to be most influential at low gas flow velocities, below about 5 m/s, cf. curve (b). The reason is that these contributions essentially cause a reduced signal-to-noise ratio SNR, where the noise is here modelled as incoherent (a random effect). Random effects do not cancel in the transit time difference, t_{1i} - t_{2i},

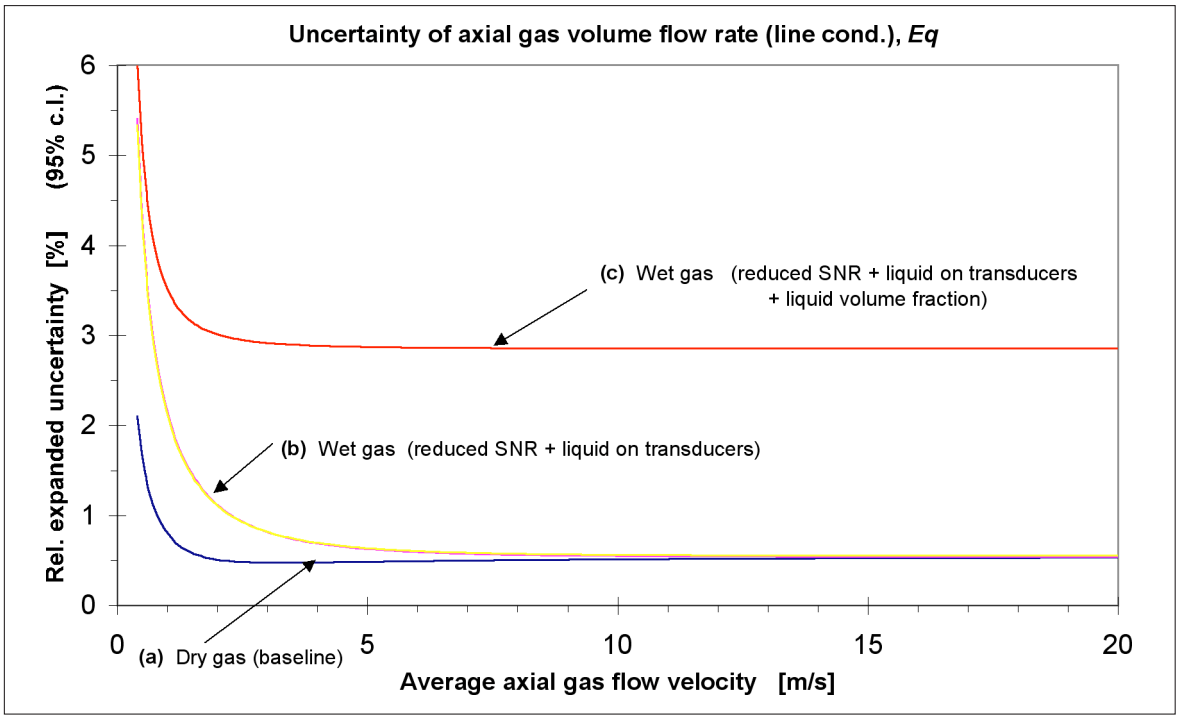

Fig. 11 Example of calculated relative expanded uncertainty, Eq, for a multipath USM, calculated using the GARUSO uncertainty model. (a) Dry gas operation (baseline example); (b) Wet gas operation (effects of increased cross-talk and sound attenuation (reduced SNR), and a 0.5 mm liquid "film" on the transducer faces); (c) Same as (b), but with additional uncertainty due to the unknown liquid volume fraction f V (assumed here to lie in the range 0-5 %). A "blind wetness correction" approach (using f V = 2.5 %) is used.

of Eq. (2), and therefore become increasingly important at low flow velocities. (In the present example the SNR is taken to be 40 dB in dry gas, and 10 dB in wet gas, corresponding to extra transit time (standard) uncertainties of 11 ns and 360 ns, respectively.)

With respect to the "wet gas contribution" (D), a 0.5 mm liquid "film" at the transducer faces has been considered in the present example. The influence on the detected transit time is here (somewhat simplified) modelled as a systematic effect, which to a large degree is cancelled in the meter (cf. Eq. (2)). The contribution to the USM uncertainty due to a 0.5 mm liquid film is thus relatively small in the present model, of the order of 0.1 %.

The "wet gas contribution" (A), $u(\hat{\phi}_V)$, is invariant to the flow velocity, and as long as this uncertainty contribution is larger than $\sqrt{E_m^2 + E_I^2}$ (which may often be the case), it contributes essentially as a constant shift of the uncertainty curve, except at the very low gas flow velocities. In the present example, the liquid volume fraction ϕ_V is not known, but is assumed to be in the range 0-5 %, and a "blind" estimate $\hat{\phi} = 2.5$ % has been used ("blind wetness correction")[2]. The standard uncertainty of the liquid volume fraction is thus taken as $u(\hat{\phi}) = 2.5\ \% / \sqrt{3} = 1.4\ \%$.

A key result from this uncertainty investigation is the following: If the liquid volume fraction is known to be less than 5 % (for instance), a relative expanded uncertainty at a level of 3 % should be a relevant perspective for USMs, by using the "blind wetness correction" approach (i.e. without knowing the actual liquid volume fraction). If the liquid volume fraction was known to be less than 1% (for instance), the relative expanded uncertainty in wet gas would be significantly lower (the uncertainty model predicts 0.8 % if the corresponding "dry gas baseline relative expanded uncertainty" was 0.5 %).

If a better estimate for the liquid volume fraction was available than in the "blind wetness correction" approach used above, the expanded uncertainty of the gas volume flow rate could be correspondingly reduced. Such results provide interesting perspectives and potentials for the use of USM in wet gas applications.

4.2 Influence of wet gas on sound velocity and attenuation

Background and motivation. Liquid contaminants in the gas may influence significantly on the sound propagating through the gas/liquid medium. Such effects are

- Scattering of ultrasound due to liquid droplets in the flow (gas-liquid aerosol, or mist),
- Increased sound attenuation (excess attenuation), due to sound scattering in the mist flow, and by liquid present on (flowing over) the transducer faces,
- Lowering of the sound velocity, due to sound scattering in the mist flow.

---

[2] *By "blind wetness correction" it is here meant that in lack of knowledge (measurement) of the liquid volume fraction ϕ, but by a tentative knowledge of the maximum value for ϕ_V, one takes the mid value in the ϕ_V interval as the estimate of ϕ_V. The standard uncertainty of this estimate is then calculated using a type B evaluation of uncertainty, and assuming a rectangular probability distribution for the variation of ϕ_V in the ϕ_V interval [ISO, 1995].*

These effects are dependent on a number of parameters, such as pressure, temperature, volume fraction, droplet size distribution, gas/liquid quality, flow velocity and the USM signal frequency. Pressures up to 200 bar and temperatures in the range from -20 to100 °C (or more) may be relevant. The liquid volume fraction may exceed 5% (cf. Section 4.1). Very limited information about typical droplet size distributions in real wet gas flow is available; - here the range 0.5 - 1000 μm has been considered. (For application at separator outlets with demistor filters, more narrow ranges may be relevant.) Signal frequencies between 100 and 200 kHz are relevant for USMs.

The investigation of these effects, and their influence on USM operation, is of interest for several reasons. Increased sound attenuation is important for USM operation, since it leads to a reduced signal-to-noise ratio (SNR), which again causes larger transit time uncertainty, and thus larger USM uncertainty. In dramatic cases, it may cause loss of acoustic path(s). A changed sound velocity, however, is not dramatic for traditional USM operation, since USMs are practically insensitive to changes in the sound velocity. On the other hand, changes in sound attenuation, sound velocity and the scattering level, - and the variation of such changes from path to path, may provide useful information about the wet gas medium. A parameter which is of particular interest in this context is the liquid volume fraction, ϕ_V. If online estimation of ϕ_V were available, that would provide possibilities to reduce the uncertainty in wet gas metering, as discussed in Section 4.1.

Basic approach. In the present section, selected attempts to investigate such influences of wet gas on the sound propagation are reported. An approach is used where one seeks improved physical insight into the mechanisms causing the effects discussed above. A combination of theoretical modelling and laboratory experiments is used for this purpose. In the laboratory experiments one seeks to test and verify candidate theoretical models. A sufficiently proven model can be used to investigate the effects of parameters such as pressure, temperature, gas/liquid quality, signal frequency, liquid volume fraction, droplet diameter, etc., on the sound propagation through the wet gas medium.

Here, the discussion is confined to the investigation of changes in sound attenuation and sound velocity due to gas-liquid aerosol (mist). Influences on the level of scattered ultrasound in gas-liquid aerosol are not discussed here.

Modelling. From the general literature on sound propagation in emulsions (liquid droplets mixed in another liquid) and gas-liquid aerosols (liquid droplets in gas), many candidate models for changes in sound velocity and attenuation in such two-phase media are available. A number of relevant models have been implemented, compared and evaluated with respect to sound propagation in gas-liquid aerosols, including effective medium models, coupled-phase models and multiple scattering models [16], [17]. These are sound propagation models used in other areas (media) and applications, which to varying extent have been verified within those areas. However, the present application of ultrasonic wet gas metering represents a new area for such models (with respect to frequency range, pressure range, temperature range, liquid volume fraction range, gas/liquid types), and the validity and applicability of the models within this area is not established. For the gas/liquid aerosols in question for wet gas metering, there is observed a significant deviation in results using the various types of models [17].

In the present paper, results using the Waterman-Truell multiple scattering model with Allegra-Hawley scattering coefficients are shown [18], [19]. This model takes into account the thermal and viscous boundary layer effects close to the droplet surface (inside and outside of the droplet), the generation of sound waves inside and outside of the droplets, and higher order oscillation modes (monopole, dipole, quadropole, etc.). The model is potentially applicable at all frequencies of relevance, from very long to very short acoustic wavelengths relative to the droplet diameter. This includes droplet resonances appearing when the acoustic wavelength is of the order of the droplet diameter.

Experiments. In the laboratory experiments reported here, an aerosol (mist) of olive oil in air, at 1 atm. and room temperature (23 °C), has been used for comparison with the Waterman-Truell multiple scattering model. The mist is generated using a TSI 9306 aerosol generator. The theory predicts increasing attenuation and increasing change in sound velo_ city for the small droplets (with largest attenuation for 0.1-1.0 mm droplets, and largest sound velocity changes for sub-mm droplets). For model testing it might then at first glance seem favourable to use droplets in the 0.1-1.0 mm range, in order to obtain larger measurable effects for the changes in sound attenuation and velocity. However, the very small droplets carry a very small portion of the total volume, so the liquid volume fraction would then be very low (sub-ppm), and the effects also relatively small. Hence, the effects of liquid droplets with a size distribution in the range of a few mm have been investigated here.

A Malvern Spraytec RTS 5000 laser diffraction system has been used for the reference measurements of droplet size distribution and liquid volume fraction ϕ_V. The Sauter mean diameter of the size distribution used here is approximately 2 mm, and the liquid volume fraction, ϕ_V, is approximately 9 ppm.

Olive oil is used to reduce evaporation effects, which for the droplet sizes in question would be significant if another liquid such as e.g. water was used. The theory indicates that the results do not vary much with liquid type, so the use of olive oil for model testing should be relevant. (Similar experiments with other liquid types such as water and Exxsol D100 have also been made, but are not reported here.)

Changes in temperature and the relative humidity (RH) were monitored during the acoustic measurements, and used to correct the measurements in the aerosol (since temperature and RH also influences on the sound attenuation and velocity).

Results. Fig. 12 shows a comparison of experimental results (markers) and modelling results (curves) for the change in sound velocity (upper plot) and the increased sound attenuation (lower plot) caused by liquid droplets in the olive-oil-in-air aerosol, plotted as a function of the liquid volume fraction, ϕ_V (up to 100 ppm = 0.01 %). The changes are shown relative to the corresponding dry gas case (air), at the same pressure, temperature, and relative humidity (RH). Three measurement series are shown, nos. 1, 2 and 3, taken over a period of more than a year. The most recent series, no. 3, is believed to be the most accurate of these, since better temperature and relative humidity measurements were available for this series, enabling a better correction for temperature and RH effects. Theoretical predictions are given for droplet diameters 0.5, 1, 2, 5, 10 and 50 μm.

For the excess sound attenuation, the agreement between the experimental results and the theory is considered to be relatively good, especially for the Series 3 measurements, which fall almost exactly on the 2 mm curve predicted by the theory. The series 1 and 2 measurements are also relatively close to the theoretical prediction, but fall more in-between the 1 and 2 mm curves. Note the increased sound attenuation which is predicted by the theory for large liquid volume fractions, and for small droplets. (For even smaller droplets than about 0.1 - 1.0 mm, the attenuation will decrease.)

With respect to sound velocity effects, precision measurement is more demanding than for the sound attenuation, due to a relatively small change in sound velocity which is observed for the liquid volume fraction and droplet sizes investigated here (which of course is an interesting result in itself). However, a reduction of the sound velocity due to the liquid droplets is measured in most cases, although the spread in measurement data is significant. In average, the series 3 data fall relatively close to the 2 mm curve. Note the increased reduction in sound velocity which is predicted by the theory for large liquid volume fractions, and for small droplets.

In Fig. 13, the Waterman-Truell model has been used to investigate the effect of increased gas pressure on the sound propagation in mist. The pressure is raised to 50 bar, while the temperature is kept constant (23 oC, as in Fig. 12). The fluids have been changed, from olive-oil-droplets-in-air to Exxsol-D80-droplets-in-methane (which is more relevant for wet gas applications). This is done since the theory predicts (not shown here) that the effect of pressure on sound attenuation and velocity is considerably larger than the temperature and fluid type effects. Droplet diameters in the range 1 - 1000 mm are simulated. Note that in Fig. 13 liquid volume fractions up to 10 % = 100000 ppm are shown, to cover a larger range than in Fig. 12. As a consequence, significantly larger scales are used in Fig. 13 for the predicted changes of sound velocity and attenuation.

A comparison of Figs. 12 and 13 reveals that the theoretical model predicts a dramatic influence of gas pressure on the excess sound attenuation and on the change in sound velocity of the gas-liquid aerosol. Increasing pressure reduces the excess attenuation and the change in sound velocity, due to reduced characteristic acoustic impedance between the gas and the liquid droplets at elevated pressures. Very large effects are predicted in some parameter ranges. For example,

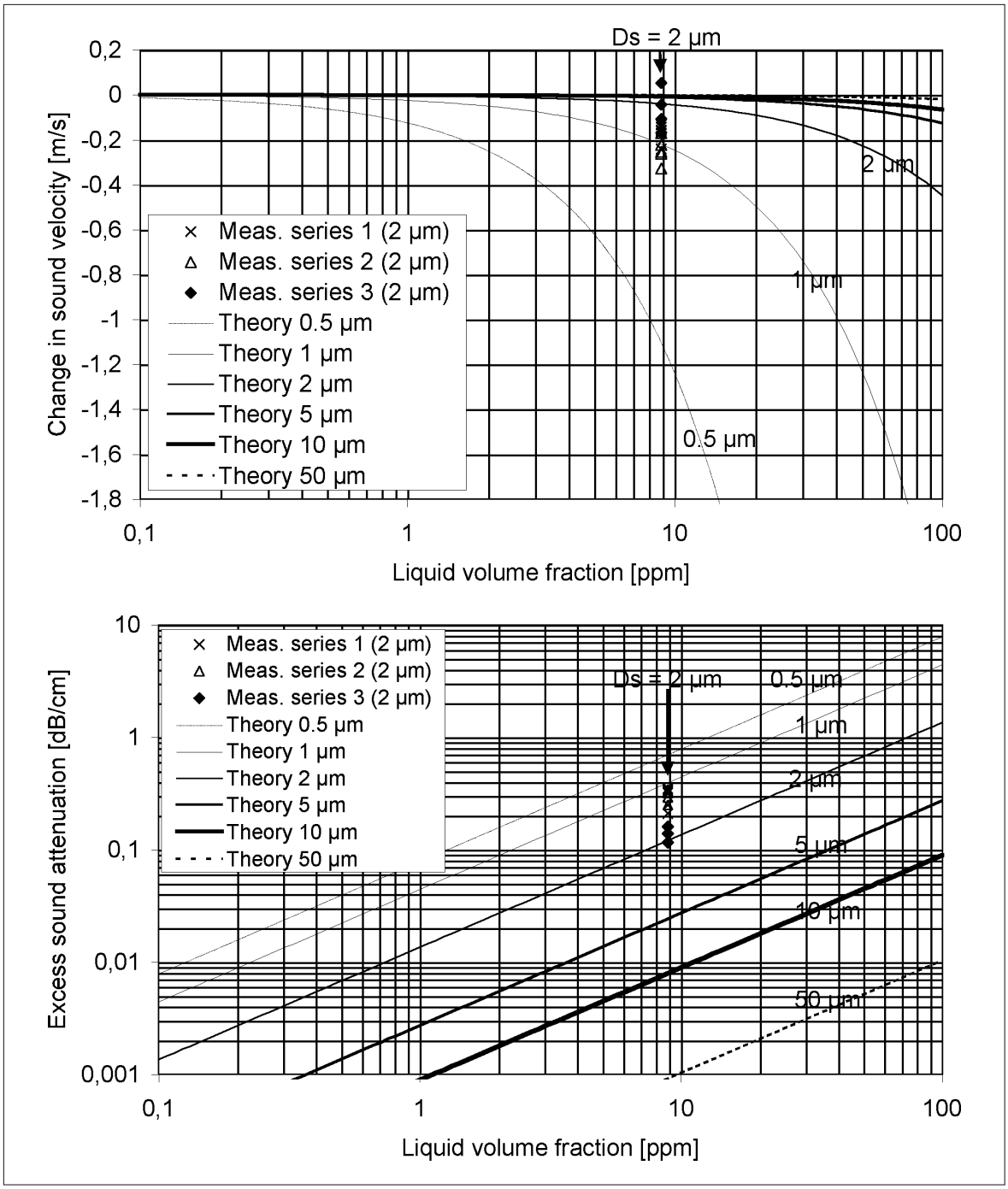

Fig. 12 Comparison of experimental results (markers) and modelling results (curves) for the change in sound velocity and attenuation caused by the liquid droplets in a gas-liquid aerosol, plotted as a function of the liquid volume fraction, ϕ_V. Static laboratory measurements with mist of 2 mm diameter droplets of olive oil in air, at 1 atm. and 23 °C.

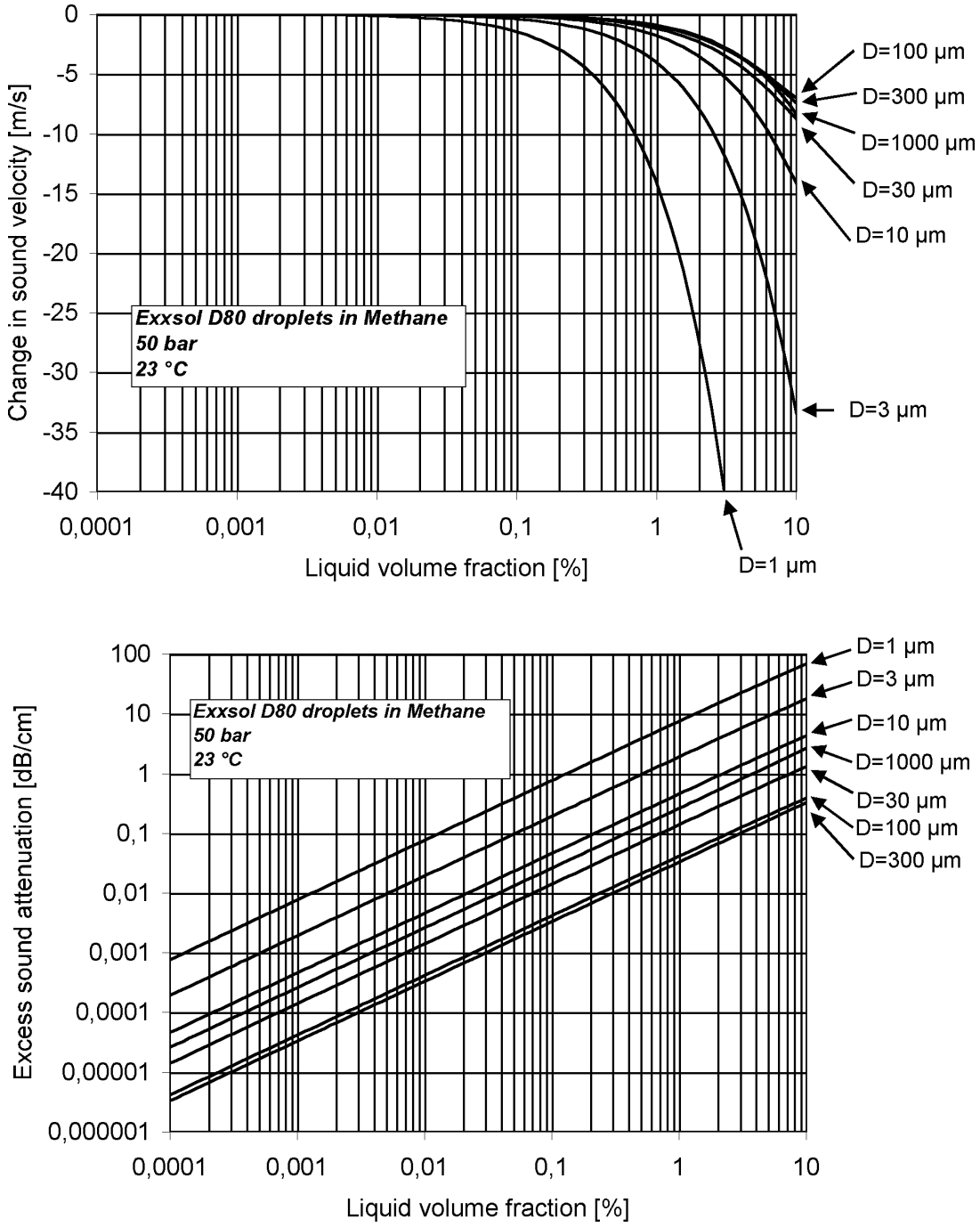

Fig. 13 Predicted change in sound velocity and attenuation using the Waterman and Truell multiple scattering model. Mist of Exxsol D80 droplets in methane, at 50 bar and 23 °C.

the excess attenuation of a 10 ppm (0.001 %) and 1 mm diameter aerosol at 1 atm. is predicted to be about 0.45 dB/cm, or 45 dB/m, which is relatively large (cf. Fig 12). At 50 bar, the excess attenuation of this aerosol is predicted to be about 0.01 dB/cm, or 1 dB/m, which is negligible. Such results have significant consequences for operation of USMs in wet gas mist flow. As mentioned above, the influence of the gas/liquid qualities and the temperature are predicted to be negligible in comparison.

It is interesting to note from these simulation results that small droplets, in the range below 1 mm, which "carry " a low liquid volume fraction, are predicted to cause the largest change in sound velocity, and the largest sound attenuation. Large droplets "carry" a higher liquid volume fraction, but are predicted to cause the least change in sound velocity, and the lowest sound attenuation.

It should be noted that the measurements shown here are results from an ongoing project, and represent preliminary results. Experimental testing and verification of theoretical models for sound attenuation and velocity in gas-liquid aerosols is indeed a challenging work, due to the relatively small effects one experiences in the parameter ranges where controlled measurements can be set up at a reasonable cost. In other parameter ranges, where the effects are larger and potentially more easily measured, experiments under controlled conditions are far more difficult to set up.

So far one may conclude that the experimental results are in fair agreement with the candidate theoretical model for sound attenuation and velocity which is investigated and used here, and support this theory. However, more measurement data points (over a larger range of liquid volume fraction, droplet diameter, pressure, temperature, etc.) are necessary to conclude on the validity of the theory.

4.3 Hardware development and flow testing

A 6" wet gas test meter using 3 acoustic paths has been developed by Kongsberg Metering and CMR, and is currently being tested in wet gas flow (natural gas and Stoddard solvent) at CEESI in Colorado, USA. Preliminary test data were obtained shortly before the deadline of this paper. The results are encouraging, but are insufficient for presentation at the time of writing. The first objective is to measure the gas volume flow rate, in spite of liquid contaminants being present, and without knowing the liquid volume fraction. Possibilities for measurement of the liquid volume fraction using ultrasonic techniques are also addressed in the project.

5. CONCLUSIONS

Results and progress from an ongoing R&D program related to the Kongsberg Metering MPU 1200 multipath ultrasonic gas flow meter have been presented. Three main topics are addressed: (1) calculation of gas density from the measured sound velocity, (2) operation at complex installation conditions (with disturbed flow velocity profiles), and (3) measurement of wet gas.

An algorithm for calculation of the gas density on basis of the sound velocity measurement output from the USM, and additional measurements of pressure and temperature, has been developed and implemented in a 6" MPU 1200. The method has been tested at Statoil’s flow laboratory K-Lab, Norway (April 1999), with deviation from the reference density measurements of typically ±0.1 %. A sensitivity analysis of the method has been carried out, indicating that more generally, the relative expanded uncertainty of the current ultrasonic density measurement method may be expected to lie in the 0.5-1 % range (within a 95 % conf. interval). However, solutions are identified which in the future may further improve this uncertainty number.

An improved integration algorithm for more robust and accurate operation of the MPU 1200 at complex installation conditions has been developed, and is to be implemented in the meter. The improvements involve only software changes in the USM, so that existing meter installations can be easily upgraded. The method has been flow tested (by post-processing) for a 6" meter (June 1999) at K-Lab, Norway, and for a 12" meter on recent (August 1999) flow test data provided by Southwest Research Institute, Texas. Significant reductions of the meter uncertainty are demonstrated in both tests, including improved robustness with respect to relevant bend configurations.

Work is underway to upgrade the MPU 1200 technology for measurement of natural gas flow that contains liquid phase contaminants (wet gas). A 3-path 6" test meter is currently being flow tested in wet natural gas at CEESI, Colorado. The GARUSO uncertainty model for ultrasonic gas meters has been further developed and used to account for wet gas effects. The influence of wet gas (liquid droplets, liquid film, etc.) on sound transmission and scattering is investigated through experimental and modelling work. Changes in sound attenuation, sound velocity and the scattering level, - and the variation of such changes from path to path, are parameters of interest for design and operation of USMs in wet gas, and may potentially provide useful information about the wet gas medium.

ACKNOWLEDGEMENTS

The authors wish to thank T. A. Grimley, Southwest Research Institute, Texas, and the Gas Research Institute, Chicago, for giving permission to use the experimental flow test data shown in Table 1 and Fig. 9, which were originally used as a basis for ref. [13]. Also they gave permission to use new (CMR - processed) results in Table 2 and 3, and Fig. 10, based on these experimental flow test data.

In addition to the authors, Andrew C. Baker, Hilde Furset, Atle A. Johannessen, Øyvind Nesse, Tore Tjomsland, Frode Johnsen and Anders Hallanger, CMR, have contributed to the work presented here.

The work has been carried out in a Joint Industry Programme between Christian Michelsen Research, Kongsberg Metering, Statoil, Norsk Hydro and Phillips Petroleum Company Norway, and has been supported by The Research Council of Norway.

REFERENCES

[1] **AGA-9:** "Measurement of gas by multipath ultrasonic meters". Transmission Measurement Committee, Report no. 9, American Gas Association (A.G.A.) (June 1998).

[2] **Wild, K.:** "A European collaboration to evaluate the application of multi-path ultrasonic gas flow meters", In: Proc. of 4th International Symposium on Fluid Flow Measurement, Denver, Colorado, USA, June 28-30, 1999.

[3] **Kristensen, B. D., Lofseik, C. and Frøysa, K.-E.:** "An overview of projects related to the KOS FMU 700 6 path ultrassonic gas flow meter", A.G.A.-98 Operations Confererence, Seattle, Washington, May 17-19, 1998.

[4] **Sakariassen, R.:** "Why we use ultrasonic gas flow meters", Proc. of the 13th North Sea Flow Measurement Workshop, Lillehammer, Norway, 1995

[5] **Watson, J.:** "A review of important gas flow measurement parameters", Practical Developments in Gas Flow Metering. One Day Seminar – 7 April 1998, National Engineering Laboratory, East Kilbride, UK.

[6] **Beecroft, D.:** "Is a wet gas (multiphase) mass flow meter just a pipe dream?", Proc. of the 16th North Sea Flow Measurement Workshop, Gleneagles Hotel, Perthshire, Scotland, 26-29 October 1998.

[7] **Tjomsland, T. and Frøysa, K.-E.:** "Calculation of natural gas density from sound velocity. Description of theory and algorithms implemented in the Deca code," CMR report no. CMR-97-F10015, Christian Michelsen Research AS, Bergen (June 1997). (Confidential.)

[8] **Starling, K. E. and Savidge, J.:** "Compressibility factors of natural gas and other related hydrocarbon gases", A.G.A. Transmission Measurement Committee, Report No. 8 (AGA-8-94); American Gas Association; 2nd ed., November 1992; 2nd printing (July 1994).

[9] **Frøysa, K.-E., Furset, H. and Baker, A. C.:** "Density and ultrasonic velocity calculations for natural gas. Sensitivity analysis of DeCa," CMR report no. CMR-98-F10002, Christian Michelsen Research AS, Bergen (December 1998). (Confidential.)

[10] **Frøysa, K.-E. and Lunde, P.:** "VESUM - Version 1.0. Uncertainty model for velocity of sound measurements for the 6-path FMU 700 ultrasonic gas flow meter," CMR report no. CMR-98-F10001, Christian Michelsen Research AS, Bergen (December 1998). (Confidential.)

[11] **Lygre, A., Johannessen, A. A., Dykesteen, E. and Norheim, R.:** "Performance test of a 6 path USM", Proc. of the 13th North Sea Flow Measurement Workshop, Lillehammer, Norway, 1995.

[12] **Grimley, T. A.:** "12 inch ultrasonic meter verification testing at the MRF ", Proc. of the 4th International Symposium on Fluid Flow Measurement, Denver, Colorado, USA, June 28-30, 1999.

[13] **Grimley, T.:** "Recent 12-inch ultrasonic meter testing at the MRF", Presented to the A.G.A. Gas Measurement Research Council, Seattle, Washington, September 14, 1999.

[14] **Lunde, P., Frøysa, K.-E. and Vestrheim, M.:** "GARUSO - Version 1.0. Uncertainty model for multipath ultrasonic transit time gas flow meters". CMR Report No. CMR-97-F10014, Christian Michelsen Research AS, Bergen (August 1997).

[15] **ISO,** "Guide to the expression of uncertainty in measurement. First edition". International Organization for Standardization, Genéve, Switzerland (1995)

[16] **Lunde, P., Frøysa, K.-E., Nesse, Ø., Vestrheim, M. and Midttveit, M.:** "Wet gas flow metering. Ultrasonic transit time methods. Basic Studies". CMR Report No. CMR-96-F10029, Christian Michelsen Research AS, Bergen (December 1996). (Confidential.)

[17] **Frøysa, K.-E. and Lunde, P.:** "Comparison of simulation models for ultrasonic propagation in wet gas", In: Proc. of 22nd Scandinavian Symposium on Physical Acoustics, Ustaoset, 31 January - 3 February 1999, edited by U. K. Kristiansen, Scientific / Technical Report No. 429904, Norwegian University of Science and Technology, Dept. of Telecommunications, Acoustics (May 1999), pp. 11-12.

[18] **Waterman, P. C. and Truell, R.:** "Multiple scattering of waves," J. Math. Phys. 2, 512-537 (1961).

[19] **Allegra, J. R. and Hawley, S. A.:** "Attenuation of Sound in Suspensions and Emulsions: Theory and Experiments", J. Acoust. Soc. Am. 51, 1545-1564 (1972).